Journal of Ultrafine Grained and Nanostructured Materials
https://jufgnsm.ut.ac.ir
Vol. 58, No.2, June 2025, pp. 143-151
Print ISSN: 2423-6845 Online ISSN: 2423-6837
DOI: 10.22059/jufgnsm.2025.02.02

Mechanical Alloying-Induced Nanostructuring and β-Ti Phase Formation in Ti-Sn-Mn and Ti-Zr-Sn-Mn Powders

Amir Hossein Gholami [1], Seyed Farshid Kashani-Bozorg [1,*], Mohammad Reza Barati [2]

[1] School of Metallurgy and Materials Engineering, College of Engineering, University of Tehran, Tehran, Iran.
[2] Department of Advanced Materials and New Technologies, Iranian Research Organization for Science and Technology (IROST), P.O. Box 33535111, Tehran, Iran.

Recieved: 7 September 2025; Accepted: 11 November 2025

[*]Corresponding author, E-mail: fkashani@ut.ac.ir

ABSTRACT

This study examines the structural evolution of Ti-5Sn-3Mn and Ti-10Zr-5Sn-3Mn (all wt. %) alloys during mechanical alloying. In the case of Ti-5Sn-3Mn, XRD results showed minor variation up to 20 h, followed by peak broadening and intensity reduction after 40 h due to grain refinement and strain accumulation. After 60 h, Sn and Mn peaks vanished, indicating their dissolution in the Ti lattice and formation of a β-Ti solid solution, while a Ti(101) peak shift confirmed change in lattice parameter. In the case of Ti-10Zr-5Sn-3Mn alloy, Zr addition promoted faster Sn dissolution and β-phase formation at shorter milling time. Both alloys developed stable nanocrystalline structures as crystallite size decreased with milling time. Moreover, a gradual reduction in particle size of the mill product occurred by increasing the milling time as revealed by scanning electron microscopy. Furthermore, particles reduction was associated with chemical homogeneity and uniform distribution.

Keywords: *Ti-based alloys, Mechanical alloying, Nanostructured materials, β/α-Ti phases, Sn-Zr-Mn.*

1. Introduction

Titanium alloys is currently one of the most sought-after materials for orthopedic equipment and bone scaffolds due to their good mechanical properties as well as an excellent biocompatibility and corrosion resistance [1, 2]. Various techniques are employed for the fabrication of titanium alloys such as casting, forging, sintering, powder metallurgy, and in recent years, additive manufacturing [3, 4]. It is important to note that among these methods, solid state powder metallurgy is capable to produce non-textured nanostructured material [5]. Nanocrystals often show properties superior to those of conventional materials with coarser structure. Such materials exhibit increased mechanical strength, enhanced diffusivity and other valuable properties as compared to coarse-grained counterparts [6].

Mechanical alloying as a solid state powder metallurgy technique is a non-equilibrium process for producing nanostructured materials, formation of a fine dispersion of second phase particles, extension of solubility limits and development of amorphous phases. The process is associated with simplicity, low cost, and large-scale capacity, which can achieve chemical and microstructural homogeneity as well as direct control over alloy composition [7-10]. Mechanical alloying has been defined as a process that involves repeated cold welding, fracturing of powder particles in a high-energy ball mill. Due to the non-equilibrium

processes involved in mechanical alloying, it is possible to dissolve elements with high vapor pressure and low solubility limits to achieve compositions with extended solid solution [8]. It has been reported in numerous studies that increasing time and milling energy leads to significant reductions in average particle size [11, 12]. It has been shown that mechanical alloying parameters can significantly impact the properties of the fabricated powder products due to the increased diffusional path and surface area of the product. Awad et al.[13] examined the different Mo powder content fabricated by elemental blended and mechanical alloying in Ti-Mo system. It was found that the microhardness and compressive properties were enhanced with Mo addition and MA fabrication by 11.5 and 27%, respectively, mainly due to solid solution strengthening, plastic deformation, high dislocations, and lattice defects. High energy ball milling of titanium not only reduces the grain size to nanometer level but also induces transformation [14, 15]. Hamadi et al. [16] investigated the effect of milling time on the structural, physical, and tribological behaviors of the nanostructured ternary Ti-25Nb-25Zr alloy prepared by high-energy milling and their results showed that increasing milling time reduced crystallite and increased the β-Ti phase fraction, resulting in spherical morphology and textured microstructure.

This study investigated the formation of solid solutions in ternary Ti-5Sn-3Mn (wt. %) and quaternary Ti-10Zr-5Sn-3Mn (wt. %) titanium based systems through mechanical alloying, focusing specifically on the role of processing time in controlling grain refinement.

2. Materials and Methods

Elemental powders of Ti (purity 99.800%, 100 μm, Merck), Sn (purity 99.000%, 60 μm, Merck), Mn (purity 99.000%, 60 μm, Merck) and Zr (purity 99.000%, 60 μm, Merck) were used. The mechanical alloying process was conducted using 140 ml steel vials and balls as grinding media of 5, 10 and 20 mm in diameter with a planetary ball mill at room temperature and vials were sealed with high purity argon (99.999%) before the fabrication process. The ball to powder weight ratio was maintained at 10:1 and the high energy ball-milling was carried out at a rotation speed of 300 rpm. Stearic acid ($C_{18}H_{36}O_2$) was added to the powder mixture as process control agent at a constant weight percent of 2 wt. % to prevent cold welding between powders and balls or vials. The crystal structure of the milled products was investigated by a Philips X' Pert Pro X-ray diffractometer (XRD) using a Cu-Kα radiation (λ=0.15406 nm) and step size of 0.02° over the 2θ range of 10-90. The crystallite size (d) and lattice strain (ε) were calculated based on X-ray peak broadening using the well-known Williamson-Hall method[17]:

$$\beta=\frac{0.9\,\lambda}{t(\cos\theta)}+\eta(\tan\theta) \quad (1)$$

where β, t, θ and η are full-width at half maximum height of the peak with maximum intensity (in radian), average crystallite size (in nm), Bragg's angle of the peak and lattice strain, respectively.

The actual broadening of the diffraction line (β_{real}) is caused by the reduction of grain size and lattice strain was calculated using Eq. 2:

$$\beta_{real}^2=\beta_{obs}^2+\beta_{ins}^2 \quad (2)$$

where, β_{obs} is the broadening observed from the pattern (measured value), and β_{ins} is the broadening related to the instrument (diffractometer).

Morphological and compositional investigation during mechanical alloying was conducted by means of a field emission scanning electron microscope (FE-SEM).

3. Results and Discussion

Figure 1 illustrates the X-ray diffraction patterns of Ti-5Sn-3Mn (wt. %) ternary system as a function of different milling times, i.e. various stages of the mechanical alloying process. The strongest Sn (200) and (101) reflections are detected at 2θ = 30.66° and 32.06°, and the strongest reflections (101) and (100) for Ti at 2θ = 40.2° and 35.2°, respectively. The peaks associated with Mn do not exhibit high intensity due to its low weight percentage in the alloy's chemical composition; however, one and only peak corresponding to Mn was identified at a 2θ = 43.2°. It has been found that the intensity and spread of Ti, and Sn peaks did not change significantly during the mechanical alloying process until 20 h. Sever plastic deformation due to mechanical alloying results in a mechanically driven crystallization process and accordingly, any amorphization in the early stages of the process is suppressed. However, after 40 h. of milling, the intensity of the alloying element peaks has generally decreased which is associated with the grain size reduction and/or accumulations of mechanical strains with increasing milling time. As a result of milling for 60 h, the Mn and Sn peaks have disappeared, which may indicate that the Mn and Sn elements have been dissolved into the Ti lattice. Thus, it can be considered that ternary Ti-5Sn-3Mn solid solution formed. Also, covering of Ti powders with finely crushed Mn and Sn particles might have occurred. As the milling time extended to 60 h, the peaks are broadened which indicated the formation of partially amorphous phase in

the milled product. This indicated the formation of fine grain and a high density of defects caused by a large local strain in the powder particles. The decreasing of Ti matrix crystallite size due to the increasing of milling time could also be due to the increasing number of collisions per unit time and consequently due to the transfer of more energy on the Ti matrix powder particles during the same milling condition. Further, a minor shift (towards smaller angle) in the position of the Ti (101) XRD peaks was also noticed and this could be related to the dissolution of alloying elements into the Ti matrix. The gradual angular shift of Ti peaks to smaller angles is mainly attributed to the formation of titanium solid solution and negligibly to increase of lattice parameter as a result of grain compression. Due to cold welding of particles and formation of a lamella structure in the mechanical alloying process, a homogenous titanium solid solution was formed. As a result, the Ti lattice parameter and subsequently the planes distance increased, followed by a diffraction angle decrease in accordance to the Bragg's law [18]. Nouri et al.[19] revealed that in the ternary Ti-Sn-Nb, a significant dissolution of Nb and Sn into Ti lattice was achieved and there were still Nb traces remained in longer mechanically alloyed powder particles. Increasing milling time led to a considerable particle refinement and the development of α-Ti and partial amorphous structure. However, with the prolonged duration of ball milling, no evidence of the β-Ti phase was observed in this ternary system. This observation may indicate the stronger influence of Mn, in the presence of Sn, on destabilizing the β phase compared to the stabilizing effect of Nb. As illustrated in the X-ray diffraction pattern, after 60 h of continuous milling, the β phase peaks of titanium were detected. These indicated that Mn acted as a beta phase stabilizer during the non-equilibrium mechanical alloying process. Although Sn is considered as a neutral element in terms of α vs. β [20] but, in the presence of a beta phase stabilizing element, it contributes to stabilizing the beta phase. With continued milling process, the intensity of the β-Ti peak increases, however, the structural system remains biphasic.

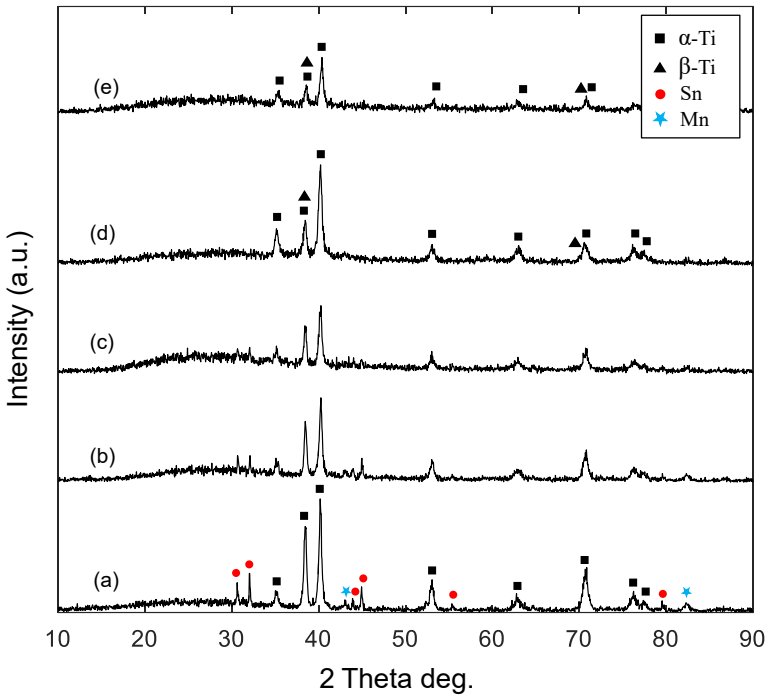

Fig. 1- XRD patterns of Ti-5Sn-3Mn (wt. %) elemental powders with 2wt. % stearic acid as a function of different milling times: (a) 0 (b) 20 (c) 40, (d) 60 and (e) 80 h.

Figure 2 illustrates the X-ray diffraction patterns of the quaternary Ti-10Zr-5Sn-3Mn (wt. %) system during the mechanical alloying process. Within the first 20 h of milling, no significant changes were observed in the peak intensities of the alloying elements, indicating that the input energy was still insufficient to promote substantial grain refinement. After 40 h, a noticeable decrease in the relative intensities of the alloying element peaks occurred, and the reflections associated with Mn and Zr nearly disappeared. Continued milling up to 60 h resulted in the disappearance of the peaks corresponding to Sn, while the β-titanium phase emerged. Beyond 60 h, no further peak broadening was detected, suggesting that the required energy for amorphization had not been reached. When compared with the ternary Ti-6Sn-3Mn system, the incorporation of Zr into the composition enhanced the dissolution of Sn at shorter milling times and accelerated the formation of the β-Ti phase. This observation highlights the significant role of Zr in stabilizing the β-Ti phase, particularly in the presence of a strong stabilizing element such as Mn. Consequently, both the thermodynamic and kinetic conditions necessary for the α-to-β titanium phase transformation were achieved within shorter milling durations.

The milling parameters of these systems provided the required energies for the formation of ternary Ti-5Sn-3Mn and quaternary Ti-10Zr-5Sn-3Mn nanostructured solid solutions, and thus, there was no need for any subsequent annealing treatment or quenching. As mechanical alloying is an entirely solid-state processing method, it is not constrained by phase diagram limitations. Therefore, solid solubility levels similar to those of rapid solidification process were attained.

The formation of solid solution is a manifestation of mechanical alloying phenomena due to severe plastic deformation of cold welded powders. The mechanical alloying process is one of the severe plastic deformation methods in which it is possible to dissolve two elements that are either immiscible or have a low solubility limit in each other. This enhancement in solubility occurs in two ways; 1-the solute element is located at the grain boundaries, as mechanical alloying is one of the methods for increasing grain boundary density through severe plastic deformation. 2-crystallites composed of different elements are formed, and dissolution subsequently occurred at their boundaries. Since the fraction of grain boundaries in nanostructured materials is increased, a high density of pathways associated with short-range diffusion exists within the material, and the diffusion rate through the grain boundaries is high. The improvement in diffusion conditions can lead to greater dissolution of immiscible elements, even at low temperatures. In addition, a slight increase in temperature during the ball milling process will enhance the diffusion of the material and consequently, it stabilizes the alloyed system and establishes conditions conducive to the formation of a homogeneous solid solution throughout the mechanical alloying process.

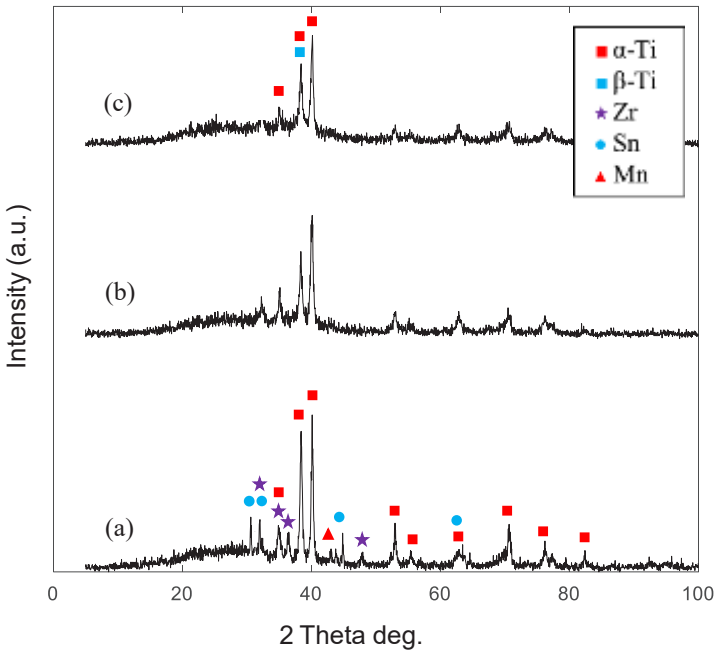

Fig. 2- XRD patterns of Ti-10Zr-5Sn-3Mn (wt%) elemental powders with 2wt% stearic acid under different milling times: (a) 20 hr, (b) 40 hr, and (c) 60 hr.

Figure 3 displays the variations of mean nanocrystallite size and microstrain of α-Ti lattice in ternary Ti-5Sn-3Mn and quaternary Ti-10Zr-5Sn-3Mn milled products using x-ray diffraction results. In general, the crystallite size of the milled powders decreases with prolonged milling time and eventually reaches a steady-state (saturation level) once a balance is established between fracturing and cold welding events during mechanical milling. This minimum crystallite size, depends on both the material and the milling parameters. The achievable minimum crystallite size is governed by the competition between plastic deformation through dislocation motion, which promotes grain refinement, and the recovery and recrystallization processes of the material, which act to increase grain size. This interplay defines the lower grain size limit attainable in pure metals and alloys. As severe plastic deformation induced by ball milling process is inherently repetitive, the accumulated strain progressively increases with extended milling time. This process enables most materials to attain a nanocrystalline structure. As shown in the figure, the crystallite size gradually decreases with increasing milling time; however, beyond a certain duration, the rate of crystallite refinement diminishes. The minimum achievable crystallite size during ball milling is governed by the balance between defect generation—such as dislocations—and their subsequent recovery. Accordingly, a higher rate of defect formation results in smaller mean crystallite size. Temperature also plays a critical role in attaining the minimum crystallite dimensions, with lower milling temperatures generally yielding finer crystallites. Furthermore, the minimum crystallite size is influenced by the material's melting point. Materials with higher melting points tend to produce finer grains, as the homologous temperature is reduced and defect recovery processes become more constrained[21].

After 40 h of milling process, a progressive equilibrium is established between the two processes of mechanical deformation (dislocation generation) and recovery/recrystallization (elimination or rearrangement of dislocations). Mn is naturally more brittle than Sn [22]. Thus, existence of Mn can increase the rate of mechanical deformation which in turn provides crystal refinement and resulting in more easily fracturing. The value of minimum crystallite size differs among various metals and is also influenced by their crystal structure. For most metals, the minimum crystallite size lies within the nanometer range. However, metals with a body-centered cubic crystal structure attain significantly smaller crystallite sizes compared to those with other crystal structures [23, 24]. This behavior is attributed to the limited capacity for extensive plastic deformation in body centered cubic metals and their consequently higher tendency to undergo fracture during milling. It was suggested that the minimum grain size is determined by the minimum crystallite size that can sustain a dislocation pile-up within a grain and by the rate of recovery [14].

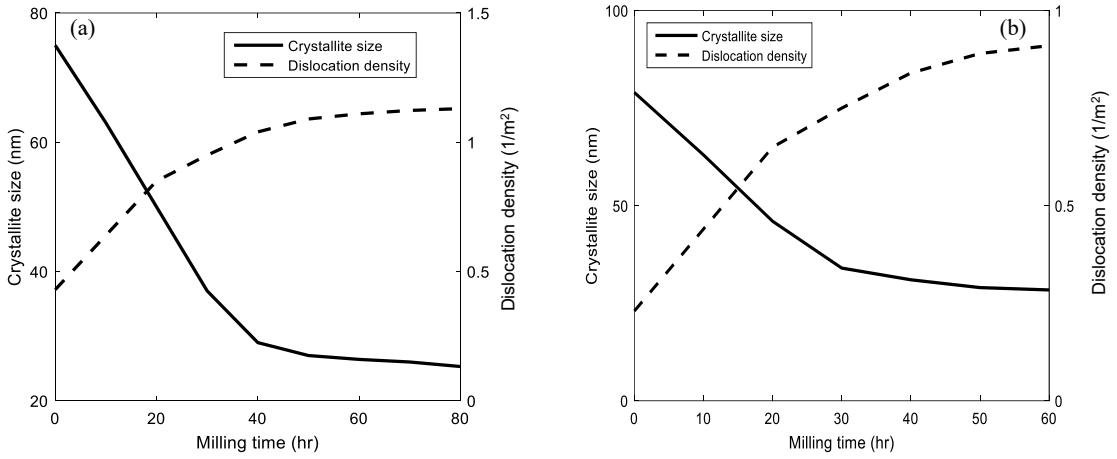

Fig. 3- Variations of α-Ti crystallite size and lattice microstrain in: (a) Ti-5Sn-3Mn and (b) Ti-10Zr-5Sn-3Mn powder products as a function of various milling times.

Based on the dislocation pile-up model, the relationship between dislocation density (ρ) and lattice strain in the mechanically alloyed powders may be calculated from the crystallite size, D, and micro-strain, ε as follows [25]:

$$\rho = \frac{2\sqrt{3}\times\varepsilon}{Db} \quad (3)$$

The X-ray diffraction results reveal that, despite prolonged milling durations, no amorphous phase formation occurred in the products. Rather, extended milling led to a relative reduction in peak intensities along with minor peak broadening. Amorphous phase transforms into a crystalline phase on continued milling after the formation of the amorphous phase, and that this phenomenon was referred to as mechanical crystallization. Crystalline phase normally has a lower free energy than the amorphous phase but its free energy can be increased by introducing a variety of crystal defects such as dislocations, grain boundaries, stacking faults, and etc. [26]. According to thermodynamic principles, amorphization occurs when the free energy of the hypothetical amorphous phase is lower than that of the corresponding crystalline phase. Thus, it is possible that the sum of the crystalline free energy and the defect energies introduced during processing surpasses the free energy of the amorphous phase. The magnitude of energy increase is different for different types of defects. As an example, increasing the dislocation density to 10^{16} /m^2 increases the free energy by about 1 kJ/mol, while decreasing the grain size down to 1 nm increases the free energy by about 10 kJ/mol [27]. The sole contribution of a solid solution to the increase in system free energy arises from grain refinement. Nevertheless, this increase is insufficient for amorphization. Mechanical alloying reduces the crystallite size to the nanometer scale and disrupts the long-range order of intermetallic compounds, thereby significantly increasing the energy of the milled powders. In fact, the energy is elevated to a level higher than that of the hypothetical amorphous phase. Under such conditions, the formation of the amorphous phase becomes thermodynamically more favorable than that of the crystalline phase. In most cases, amorphization has been observed through the mechanical alloying method, while alloys with a low solute atomic concentration usually cannot be transformed into the amorphous state. Overall, if the phase diagram indicates a broad solid solution compositional range, amorphization becomes less feasible. In contrast, the presence of numerous intermetallic phases in the phase diagram enhances the tendency toward amorphization[28].

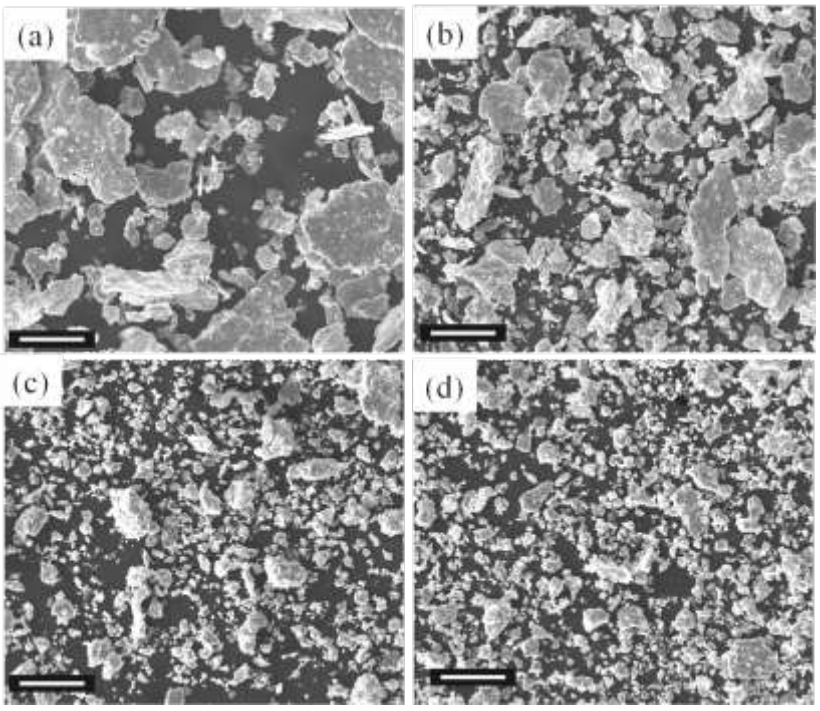

Fig. 4- SEM images of Ti-10Zr-5Sn-3Mn quaternary powder mixture after various milling times of (a) 0, (b) 20, (c) 40 and (d) 60 hr. (Scale bar = 50 μm).

In order to investigating the effect of the mechanical alloying process on the morphology of powder particles, SEM images at different milling times were utilized for quaternary Ti-10Zr-5Sn-3Mn system (Figure 4). As can be seen, particle size progressively decreases with prolonged milling time. At the early stages of milling, the raw material powders are readily deformed by compressive forces, transforming into thin lamellae, while the relatively brittle particles show resistance to such deformation and during this stage of ball milling, a large number of particles largely preserved their original shapes due to the relatively low collision energy they experienced. In contrast, after 20 hours of milling, the ductile powders began to agglomerate into larger clusters and were flattened into more platelet- or flake-like morphologies. Therefore, brittle particles are less deformed and ductile particles cause connection between brittle particles. This difference in particle deformability is responsible for the broad particle size distribution of the milled products after relatively shorter milling times.

As the ball milling process continued up to 40 hours, a multilayered structure was formed through repeated fracturing and cold welding of the flattened flakes on a fine scale. At this stage, the particles exhibited a more uniform distribution and reduced size. However, with extended milling time of 40 to 60 hours, the particles progressively transformed into an equiaxed and fine morphology. After 60 hours of ball milling, the powders exhibited a cluster-like morphology composed of multiple fine particles with an average diameter of approximately 7-10 μm. The formation of these agglomerated particles can be attributed to the dominance of the cold welding mechanism over particle fracturing during prolonged milling. Upon extending the ball milling time, the process control agent (PCA) undergoes complete decomposition, with its decomposition products subsequently integrating into the powder particles. Consequently, the PCA

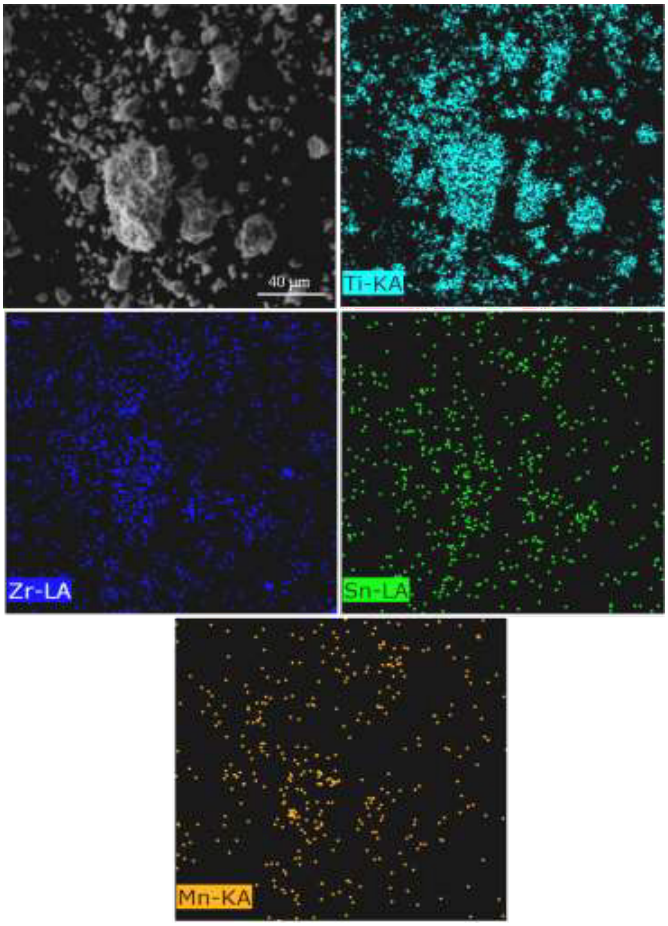

Fig. 5- X-ray map of various element of quaternary Ti-10Zr-5Sn-3M milled product after 60 hr. of milling.

becomes ineffective in suppressing excessive cold welding among the powders. When the milling time exceeds 60 hours, a dynamic equilibrium is established between the opposing mechanisms of cold welding and fracturing. It is noteworthy that particle agglomeration predominantly occurs during the initial 20 hours of milling, while continued milling from 40 to 60 hours leads to a gradual refinement and homogenization of the powder particles[29]. Thus, as the milling time increases, a more uniform particle size distribution is obtained and the probability of achieving a homogeneous chemical composition within the particles increases (Figure 5).

4. Summary

In this study, the structural evolution and phase formation of ternary Ti-5Sn-3Mn (wt. %) and quaternary Ti-10Zr-5Sn-3Mn (wt. %) powder mixtures during mechanical alloying were systematically investigated. The results demonstrated that the gradual interdiffusion of alloying elements under severe plastic deformation led to the development of nanostructured β/α-Ti solid solutions with increased lattice microstrain. The incorporation of Mn acted as a strong β-phase stabilizer, while Zr enhanced the dissolution of Sn and promoted the α-to-β phase transformation at shorter milling times. The fabrication of medical implants composed of β-Ti, which exhibit a lower elastic modulus and higher biocompatibility compared to the α phase, can enhance load transfer to the bone and mitigate the stress shielding effect. Extended milling resulted in a progressive refinement of crystallite size, reaching the nanometer scale, and promoted homogeneous particle size distribution and chemical composition. Overall, mechanical alloying proved to be an effective method for producing nanostructured ternary and quaternary Ti-based alloys with enhanced β-phase stability, demonstrating its potential as a solid-state processing route for the design of advanced titanium alloys suitable for biomedical and structural applications.

References

1. M. Long and H. J. Rack, "Titanium alloys in total joint replacement—a materials science perspective," Biomaterials, vol. 19, no. 18, pp. 1621-1639, 1998/09/01/ 1998.
2. M. Niinomi, M. Nakai, and J. Hieda, "Development of new metallic alloys for biomedical applications," Acta Biomaterialia, vol. 8, no. 11, pp. 3888-3903, 2012/11/01/ 2012.
3. K. Moeinfar, F. Khodabakhshi, S. F. Kashani-bozorg, M. Mohammadi, and A. P. Gerlich, "A review on metallurgical aspects of laser additive manufacturing (LAM): Stainless steels, nickel superalloys, and titanium alloys," Journal of Materials Research and Technology, vol. 16, pp. 1029-1068, 2022/01/01/ 2022.
4. W. Chen et al., "Controlling the microstructure and mechanical properties of a metastable β titanium alloy by selective laser melting," Materials Science and Engineering: A, vol. 726, pp. 240-250, 2018/05/30.
5. P. Bhattacharya, P. Bellon, R. S. Averback, and S. J. Hales, "Nanocrystalline TiAl powders synthesized by high-energy ball milling: effects of milling parameters on yield and contamination," Journal of Alloys and Compounds, vol. 368, no. 1, pp. 187-196, 2004/04/14/ 2004.
6. S. Haghighat-Shishavan and F. Kashani Bozorg, "Nano-Crystalline Mg (2-x) MnxNi Compounds Synthesized by Mechanical Alloying: Microstructure and Electrochemistry," Journal of Ultrafine Grained and Nanostructured Materials, vol. 47, no. 1, pp. 43-49, 2014.
7. M. J. Phasha, A. S. Bolokang, and P. E. Ngoepe, "Solid-state transformation in nanocrystalline Ti induced by ball milling," Materials Letters, vol. 64, no. 10, pp. 1215-1218, 2010/05/31/ 2010.
8. A. Ebrahimi-Purkani and S. F. Kashani-Bozorg, "Nanocrystalline Mg2Ni-based powders produced by high-energy ball milling and subsequent annealing," Journal of Alloys and Compounds, vol. 456, no. 1, pp. 211-215, 2008/05/29/ 2008.
9. R. Abbasi and S. F. Kashani-Bozorg, "Electrochemical and kinetic performance of amorphous/nanostructured TiNi-based intermetallic compound with Nb substitution synthesized by mechanical alloying," Journal of Materials Research, vol. 33, no. 22, pp. 3774-3784, 2018.
10. M. Nazarian-Samani, A. R. Kamali, M. Nazarian-Samani, and S. F. Kashani-Bozorg, "Evolution and Stability of a Nanocrystalline Cu3Ge Intermetallic Compound Fabricated by Means of High Energy Ball Milling and Annealing Processes," Metallurgical and Materials Transactions A, vol. 46, no. 1, pp. 516-524, 2015/0.
11. C. Salvo, C. Aguilar, R. Cardoso-Gil, A. Medina, L. Bejar, and R. V. Mangalaraja, "Study on the microstructural evolution of Ti-Nb based alloy obtained by high-energy ball milling," Journal of Alloys and Compounds, vol. 720, pp. 254-263, 2017/10/05/ 2017.
12. S. Garroni, S. Soru, S. Enzo, and F. Delogu, "Reduction of grain size in metals and metal mixtures processed by ball milling," Scripta Materialia, vol. 88, pp. 9-12, 2014/10/01/ 2014.
13. A. H. Awad, H. A. Aly, and M. Saood, "Physical, mechanical, and corrosion properties of Ti–12Mo and Ti–15Mo alloys fabricated by elemental blend and mechanical alloying techniques," Materials Chemistry and Physics, vol. 312, p. 128661, 2024/01/15/ 2024.
14. S. F. K. Bozorg and A. Rabiezadeh, "Evolution of Nano-structured Products in Mechanical Alloying of Ni and Ti with or without Process Control Agent," AIP Conference Proceedings, vol. 1136, no. 1, pp. 825-829, 2009.
15. A. Zali, S. F. Kashani-Bozorg, Z. Lalegani, and B. Hamawandi, "Fabrication of TiFe-Based Electrodes Using High-Energy Ball Mill with Mn Additive for NiMH Batteries," Batteries, vol. 8, no. 10.
16. F. Hamadi et al., "Effect of milling time on structural, physical and tribological behavior of a newly developed Ti-Nb-Zr alloy for biomedical applications," Advanced Powder Technology, vol. 35, no. 1, p. 104306, 2024/01/01/ 2024.
17. G. Williamson and W. Hall, "X-ray line broadening from filed aluminium and wolfram," Acta metallurgica, vol, no. 1, pp. 22-31, 1953.
18. Y. Liu and W. Liu, "Mechanical alloying and spark plasma sintering of the intermetallic compound Ti50Al50," Journal of Alloys and Compounds, vol. 440, no. 1, pp. 154-157, 2007/08/16/ 2007.
19. A. Nouri, J. Lin, Y. Li, Y. Yamada, P. Hodgson, and C. Wen, "Microstructure evolution of TI-SN-NB alloy prepared by mechanical alloying," Materials Forum, vol. 31, pp. 67-70, 01/01 2007.
20. N. L. Okamoto, F. Brumbauer, M. Luckabauer, W. Sprengel, R. Abe, and T. Ichitsubo, "Why is neutral tin addition necessary for biocompatible β-titanium alloys?–Synergistic effects of

suppressing ω transformations," Acta Materialia, vol. 273, p. 119968, 2024/07/01/ 2024.
21. K. Edalati and Z. Horita, "Significance of homologous temperature in softening behavior and grain size of pure metals processed by high-pressure torsion," Materials Science and Engineering: A, vol. 528, no. 25-26, pp. 7514.
22. Y. Kusano, T. Inamura, H. Kanetaka, S. Miyazaki, and H. Hosoda, "Phase constitution and mechanical properties of Ti-(Cr, Mn)-Sn biomedical alloys," in Materials Science Forum, 2010, vol. 654: Trans Tech Publ, pp. 2118-2121.
23. C. Suryanarayana, "Mechanical alloying: a critical review," Materials Research Letters, vol. 10, no. 10, pp. 619-647, 2022.
24. D. Nafday, S. Sarkar, P. Ayyub, and T. Saha-Dasgupta, "A Reduction in Particle Size Generally Causes Body-Centered-Cubic Metals to Expand but Face-Centered-Cubic Metals to Contract," ACS Nano, vol. 12, no. 7, pp. 7246-7252, 2018/07/24 2018.
25. S. Sheibani, S. Heshmati-Manesh, and A. Ataie, "Structural investigation on nano-crystalline Cu–Cr supersaturated solid solution prepared by mechanical alloying," Journal of Alloys and Compounds, vol. 495, no. 1, pp. 59-62, 2010/04/09/ 2010.
26. Y. Cho and C. Koch, "Mechanical milling of ordered intermetallic compounds: the role of defects in amorphization," Journal of alloys and compounds, vol. 194, no. 2, pp. 287-294, 1993.
27. F. S. Froes, C. Suryanarayana, K. Russell, and C.-G. Li, "Synthesis of intermetallics by mechanical alloying," Materials Science and Engineering: A, vol. 192, pp. 612-623, 1995.
28. C. Suryanarayana, "Phase formation under non-equilibrium processing conditions: rapid solidification processing and mechanical alloying," Journal of Materials Science, vol. 53, no. 19, pp. 13364-13379, 2018.
29. S. Kleiner, F. Bertocco, F. Khalid, and O. Beffort, "Decomposition of process control agent during mechanical milling and its influence on displacement reactions in the Al–TiO2 system," Materials Chemistry and Physics, vol. 89, no. 2-3, pp. 362-366.